Molecular Biology of the Cell
Vol. 11, 3689–3702, November 2000

Bud6 Directs Sequential Microtubule Interactions with the Bud Tip and Bud Neck during Spindle Morphogenesis in *Saccharomyces cerevisiae*

Marisa Segal,* Kerry Bloom,† and Steven I. Reed*‡

*Department of Molecular Biology, The Scripps Research Institute, La Jolla, California 92037; and
†Department of Biology, University of North Carolina, Chapel Hill, North Carolina 27599

Submitted June 7, 2000; Revised August 8, 2000; Accepted August 18, 2000
Monitoring Editor: Douglas Koshland

In budding yeast, spindle polarity relies on a precise temporal program of cytoplasmic microtubule–cortex interactions throughout spindle assembly. Loss of Clb5-dependent kinase activity under conditions of attenuated Cdc28 function disrupts this program, resulting in diploid-specific lethality. Here we show that polarity loss is tolerated by haploids due to a more prominent contribution of microtubule–neck interactions to spindle orientation inherent to haploids. These differences are mediated by the relative partition of Bud6 between the bud tip and bud neck, distinguishing haploids from diploids. Bud6 localizes initially to the bud tip and accumulates at the neck concomitant with spindle assembly. *bud6*Δ mutant phenotypes are consistent with Bud6's role as a cortical cue for cytoplasmic microtubule capture. Moreover, mutations that affect Bud6 localization and partitioning disrupt the sequential program of microtubule–cortex interactions accordingly. These data support a model whereby Bud6 sequentially cues microtubule capture events at the bud tip followed by capture events at the bud neck, necessary for correct spindle morphogenesis and polarity.

INTRODUCTION

Correct orientation of the mitotic spindle along a polarity axis is critical in asymmetric cell divisions. This process is of particular importance during embryonic development when regulated spindle orientation in response to positional cues dictates asymmetry to generate daughter cells differing in developmental fate (Rhyu and Knoblich, 1995).

The budding yeast *Saccharomyces cerevisiae* divides asymmetrically, thus serving as a model for elucidating factors required for correct spindle orientation. In yeast, nuclear division between mother and daughter cells depends on the preanaphase orientation of the mitotic spindle along the mother-daughter polarity axis defined initially by the site of bud emergence.

Coordination of spindle assembly and orientation is pivotal to preanaphase spindle positioning. Both aspects of spindle development are regulated by the spindle pole body (SPB; the yeast microtubule-organizing center). SPBs organize cytoplasmic and intranuclear microtubules throughout the cell cycle (Byers and Goetsch, 1975; Hoyt and Geiser, 1996). As cells progress through the G1/S transition, the SPB is duplicated (Byers, 1981; Lew *et al.*, 1997). Once DNA replication is completed, SPBs separate and a short intranuclear spindle forms. Spindle polarity is already evident during SPB separation (Vallen *et al.*, 1992), and results in a distinct pattern of cytoplasmic microtubule–cortex interactions throughout assembly: either with the bud cortex ($SPB_{daughter}$) or the bud neck region (SPB_{mother}), respectively (Segal *et al.*, 2000). These dynamic interactions play a critical role in spindle orientation (Carminati and Stearns, 1997; Shaw *et al.*, 1997). As a result, the spindle positions at the bud neck with one SPB directed toward the mother and the other toward the daughter cell, a hallmark of correctly specified SPB fate.

We have previously shown that Clb5-dependent kinase activity is necessary to ensure that SPBs become asymmetric regarding their ability to promote the program of specific microtubule–cortex interactions in temporal coordination with spindle assembly. Loss of Clb5-dependent kinase under limiting Cdk activity (*cdc28-4 clb5*Δ at permissive temperature) results in the formation of symmetric spindles with both poles interacting primarily with the bud cortex. This leads to a terminal phenotype of cells arrested with a short spindle positioned in the bud (Segal *et al.*, 2000). Interestingly, such loss of spindle polarity resulted in lethality solely in diploids and was tolerated by haploids. Of the genetically determined characteristics associated with diploid versus haploid cells, budding pattern (Chant and Pringle, 1995; Zahner *et al.*, 1996) best correlated with determining lethality in this system (Segal *et al.*, 1998). Haploid

‡ Corresponding author. E-mail address: sreed@scripps.edu.
Abbreviations used: SPB, spindle pole body.

Table 1. List of strains

Strain	Relevant Genotype
MY1	*MATa ura3 ade1 trp1 his2 arg4 leu2*
MY2	*MATa/α ura3/ura3 ade1/ade1 trp1/trp1 his2/his2 arg4/arg4 leu2/leu2*
MYT126	*MATa cdc28-4 clb5::ARG4 HIS3:GFP:TUB1-URA3::ura3*
MYT1010	*MATa/α cdc28-4/cdc28-4 GAL1:CLB5-TRP1/trp1 HIS3:GFP:TUB1-URA3::ura3/ura3*
MYT1416	*MATa/α cdc28-4/cdc28-4 clb5::ARG4/clb5::ARG4 GAL1:CLB5-TRP1/trp1 HIS3:GFP:TUB1-URA3::ura3/ura3*
MYC1	*MATa bni1::KAN^R*
MYC11	*MATa/α bni1::KAN^R/bni1::KAN^R*
MYC4	*MATa bud3::KAN^R*
MYC1T	*MATa bni1::KAN^R HIS3:GFP:TUB1-URA3::ura3*
MYC2T	*MATa bud6::KAN^R HIS3:GFP:TUB1-URA3::ura3*
MYC3T	*MATa kar9::KAN^R HIS3:GFP:TUB1-URA3::ura3*
MYC101T	*MATa bni1::KAN^R bud6::KAN^R HIS3:GFP:TUB1-URA3::ura3*
MYC102T	*MATa bni1::KAN^R kar9::KAN^R HIS3:GFP:TUB1-URA3::ura3*
MY15DBG	*MY1 [BUD6:GFP-URA3]*
MY15DdBG	*MY2 [BUD6:GFP-URA3]*
MYC1BG	*MYC1 [BUD6:GFP-URA3]*
MYC11BG	*MYC11 [BUD6:GFP-URA3]*
MYC4BG	*MYC4 [BUD6:GFP-URA3]*
MY10CT	*MATa cdc28-4 GAL1:CLB5-TRP1::trp1 HIS3:GFP:TUB1-URA3::ura3*
MY10CC2T	*MATa cdc28-4 bud6::KAN^R GAL1:CLB5-TRP1::trp1 HIS3:GFP:TUB1-URA3::ura3*
MY16CT	*MATa cdc28-4 clb5::ARG4 GAL1:CLB5-TRP1::trp1 HIS3:GFP:TUB1-URA3::ura3*
MY16CTC2	*MATa cdc28-4 clb5::ARG4 bud6::KAN^R GAL1:CLB5-TRP1::trp1 HIS3:GFP:TUB1 URA3::ura3*
MYT1614C1	*MATa/α cdc28-4/cdc28-4 clb5::ARG4/clb5::ARG4 bni1::KAN^R/bni1::KAN^R GAL1:CLB5-TRP1/trp1 HIS3:GFP:TUB1-URA3/ura3*

*cdc28-4 clb5*Δ cells budding bipolarly (a/α diploid budding pattern) by virtue of a *bud3* mutation (Chant and Herskowitz, 1991), displayed comparable lethality to that of *cdc28-4 clb5*Δ diploids. This suggested that differences related to the haploid-diploid budding pattern affected the penetrance of the positioning defect arising from symmetrically formed spindles (Segal *et al.*, 1998).

Here we have investigated the source of this difference. Digital imaging microscopy analysis indicates that the relative contribution of microtubule interactions with the bud neck versus the bud tip, responsible for spindle orientation, differs between haploids and diploids. We further provide genetic and cytological evidence suggesting that this difference is mediated by the distinct partition of a cortical cue, Bud6, between the neck region and bud surface at the time of spindle assembly. Specifically, sequential appearance of Bud6 at the bud tip and neck regions enforces a temporal program of cytoplasmic microtubule interactions that ensures correct fate of the $SPB_{daughter}$ and SPB_{mother}, respectively. More prominent partition of Bud6 to the neck region in haploids, leading to enhanced cytoplasmic microtubule–neck interactions, accounts for the differential penetrance of the *cdc28×clb5* lethal phenotype in haploids versus diploids.

MATERIALS AND METHODS

Yeast Strains, Genetic Procedures, Media, and Growth Conditions

Strains used in this study are listed in Table 1. All strains were isogenic to 15Dau, a derivative of BF264-15D (Segal *et al.*, 1998). Deletion of *BNI1, BUD6, KAR9*, and *BUD3* was constructed by replacing the entire open reading frames using *KAN*^{R} cassettes amplified by polymerase chain reaction (PCR) according to Wach *et al.* (1994). Deletions were confirmed in all final strains by PCR analysis. Derivatives expressing a green flourescent protein (GFP)-Tub1 or a GFP-Bud6 fusion were obtained by transformation with pAFS91 (Straight *et al.*, 1997) or pRB2190 (Amberg *et al.*, 1997), respectively. Standard yeast media and genetic procedures were used (Sherman *et al.*, 1986). Yeast cultures were grown at 23°C unless indicated.

Digital Imaging Microscopy in Live Cells Expressing GFP-TUB1 or GFP-BUD6

Cells were grown to ~5×10^6 cells/ml in selective glucose-containing medium unless indicated. Cells were then mounted in the same medium containing 25% gelatin to perform time-lapse recordings at room temperature as described (Shaw *et al.*, 1997; Maddox *et al.*, 1999; Segal *et al.*, 2000). Briefly, a total of five fluorescence images was acquired at a Z-distance of 0.75 μm between each plane. A single bright field image was taken in the middle focal plane. This acquisition regime was repeated at 30- or 60-s intervals. Images were processed as previously described (Shaw *et al.*, 1997; Maddox *et al.*, 1999) by using Metamorph (Universal Imaging) software. Quantitation of cytoplasmic microtubule contacts to the neck region was carried out by scoring time-lapse digital frames of individual cells from the time of SPB separation. Mean values correspond to the total number of contacts reaching the neck in all time-lapse frames counted, divided by the total number of frames scored for each series (expressed as contacts with the neck/frame ± SD; n = number of individual cells examined). Contacts were scored for >30 min in mutant cells. In the case of wild-type cells, contacts were scored during the initial 15 min after SPB separation. The operational definition of neck region, for the purpose of microscopy, was the cell cortex area within a 0.5-μm distance from the point of constriction between the mother and the bud.

Still cell images were captured by using 100% incident light intensity and 500-ms exposures (Segal *et al.*, 1998). Strains requiring a *GAL1:CLB5* construct for viability were grown in selective 3%

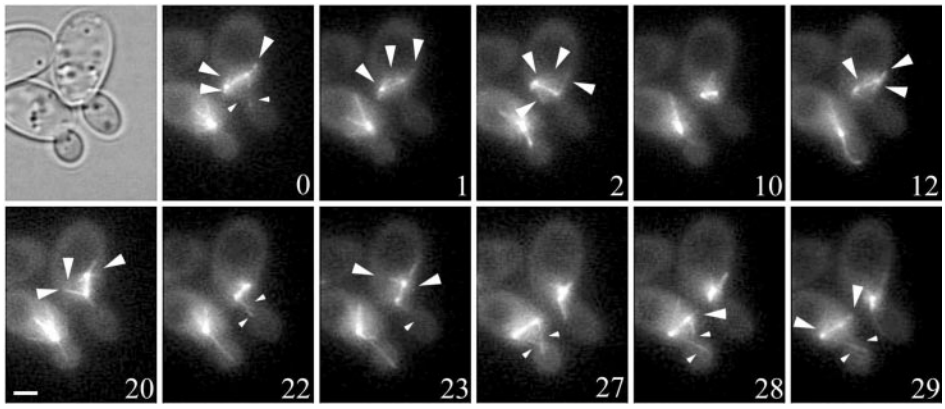

Figure 1. Cytoplasmic microtubule behavior after spindle assembly in *cdc28-4 clb5* haploids. Selected frames from a 35-min time-lapse series showing spindle orientation in *cdc28-4 clb5* haploids expressing a GFP-Tub1 fusion (MYT126). Cytoplasmic microtubules emerging from either SPB interacted with the bud tip surface (small arrowheads), reflecting lack of spindle polarity as previously described for diploids (Segal *et al.*, 2000). In addition, prominent neck interactions (large arrowheads) contributed to retention of the spindle at the neck. Neck region was defined as the cortex area within 0.5-μm distance of the point of constriction between the mother cell and the bud. Numbers indicate time elapsed in minutes. Bar, 2 μm.

galactose-0.1% dextrose medium and collected by filtration for a 6-h shift on selective glucose medium at 23°C to repress *CLB5* expression before microscopy. Quantitation of spindle morphologies and positioning was based on counting at least 500 cells at each spindle morphological stage described. Spindle measurements in digital images were carried out as previously described (Segal *et al.*, 1998).

RESULTS

Spindle Polarity and Positioning in cdc28-4 clb5 *Haploids*

We have previously shown that *cdc28-4 clb5*Δ diploids fail to confer correct fate to the SPB otherwise destined to remain in the mother cell (SPB_{mother}). The resulting disruption of polarity causes both poles to become daughter-bound, leading to the terminal translocation of the spindle into the bud at permissive temperature (Segal *et al.*, 2000). Spindle polarity was equally disrupted in haploid *cdc28-4 clb5*Δ cells. Yet, mutant haploids were viable and were rarely blocked in cell cycle progression with the spindle positioned in the bud (Segal *et al.*, 1998). This suggested that haploids and diploids may differ in some fundamental aspect of the process of spindle orientation.

To address the underlying reason for this difference, we examined cytoplasmic microtubule–cortex interactions mediating spindle orientation in *cdc28-4 clb5*Δ haploids expressing a GFP-Tub1 (α-tubulin) fusion, as was previously done for diploid cells (Segal *et al.*, 2000). As shown in Figure 1, cells assembled spindles exhibiting cytoplasmic microtubule attachments from both poles with the bud cortex (0 min, right cell and 27 min, left cell; small arrowheads). However, additional interactions between either pole and the bud neck region (Figure 1, large arrowheads), not prominent in diploid cells (Segal *et al.*, 2000), resulted in the retention of the spindle at the neck. Based on time-lapse analysis (see MATERIALS AND METHODS) we determined that 2.9 ± 1.5 contacts with the neck region occurred per time-lapse frame in haploids (n = 10 cells) compared with 0.5 ± 0.7 in diploids (n = 9 cells) >30 min after spindle assembly. The effect of cell type on the *cdc28-4 clb5* terminal phenotype indicated that translocation of the spindle across the neck constituted the critical determinant of *cdc28-4 clb5*Δ diploid lethality (Segal *et al.*, 1998). The difference in spindle–neck interactions between haploids and diploids was also apparent in parental *cdc28-4* as well as wild-type cells, neither of which exhibits the symmetric spindle phenotype. We scored 2.5 ± 1 cytoplasmic microtubule contacts with the neck region per time-lapse frame in wild-type haploids (n = 6 cells) compared with 0.9 ± 0.8 in wild-type diploids (n = 6 cells) during the first 15 min after SPB separation. A more predominant role for the neck region in spindle orientation in haploids was also consistent with the differential penetrance of spindle-positioning defects observed when comparing *dhc1*Δ (Eshel *et al.*, 1993; Li *et al.*, 1993) or *num1*Δ (Farkasovsky and Kuntzel, 1995) mutant haploids versus diploids (our unpublished results). Taken together, these results indicate that cytoplasmic microtubule–bud neck interactions contributing to spindle positioning are more prevalent in haploid relative to diploid cells.

Cortical Cues contributing to Spindle–Cortex Interactions: Localization of GFP-Bud6 in Haploids versus Diploids

Several cortical components have been implicated in spindle orientation (Farkasovsky and Kuntzel, 1995; Miller and Rose, 1998; Lee *et al.*, 1999; Miller *et al.*, 1999). Among them, we focused on Bud6 and Bni1 because of their parallel effect on budding pattern (Zahner *et al.*, 1996). The formin Bni1 localizes to the bud tip and tip of mating projections and constitutes a target of the yeast-polarizing machinery regulating actin organization (Jansen *et al.*, 1996; Kohno *et al.*, 1996; Evangelista *et al.*, 1997; Imamura *et al.*, 1997; Fujiwara *et al.*, 1998). The carboxy-terminal domain of Bni1 interacts with Bud6 (Amberg *et al.*, 1997; Evangelista *et al.*, 1997) and is essential for Bni1 function in bud site selection and spindle orientation (Lee *et al.*, 1999).

Localization of Bud6 in vegetative cells has been reported solely for wild-type diploids (Amberg *et al.*, 1997). Thus, possible differences between haploid and diploid cells underlying a differential role for Bud6 in spindle orientation were not previously addressed. We therefore compared the localization of the same GFP-Bud6 fusion (Amberg *et al.*, 1997) in haploids and diploids by time-lapse microscopy (Figure 2). In haploids, Bud6 initially associated with the prebud site and concentrated at the tip of the bud (Figure

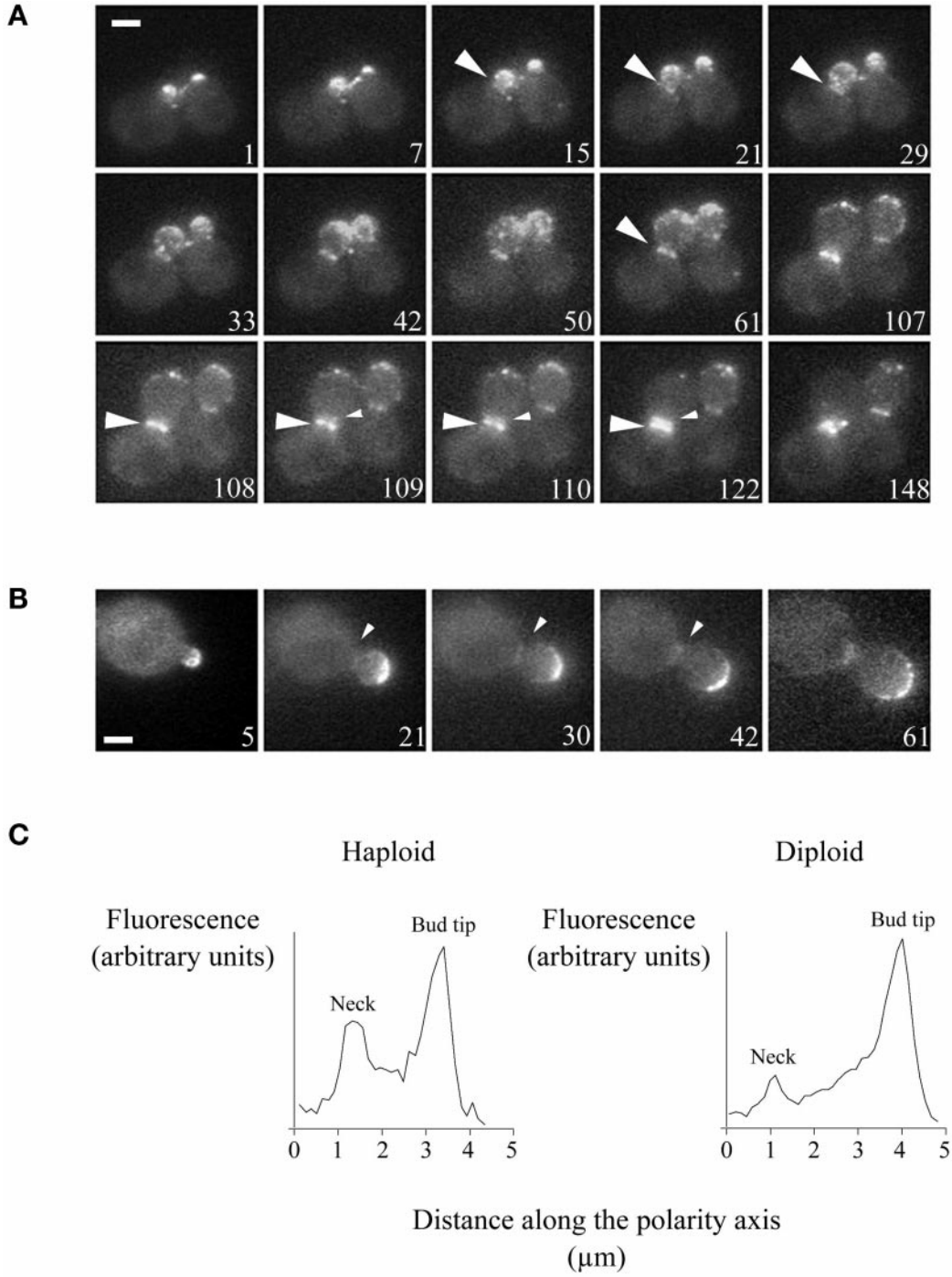

Figure 2. GFP-Bud6 localization during the cell cycle in wild-type haploids or diploids. (A) Selected frames from a 153-min time-lapse series showing representative stages of GFP-Bud6 localization in wild-type haploids (MY15DBG) during the cell cycle. Bud6 initially localized to the prebud site. Association to the neck area occurred at ~15 min after bud emergence (left cell, large arrowhead). Appearance of a second ring at the daughter face of the neck occurred at ~110 min (small arrowhead). Numbers indicate time in minutes relative to bud emergence for the cell on the left. Precise timing of label association to the cell on the right could not be determined because the growing bud on the left pushed the cell neck off focus. Bar, 2 μm. (B) Selected frames from a 169-min time-lapse series showing initial association of GFP-Bud6 to the bud tip followed by faint labeling of the neck region (arrowhead) in a wild-type diploid (MY15DdBG). Label on the bud surface remained concentrated at the distal portion of the bud until 30 min before cytokinesis. Numbers indicate time relative to bud emergence. Bar, 2 μm. (C) Plot showing linescans through the polarity axis reflecting the relative association of GFP-Bud6 to the neck and bud surface in a haploid or diploid wild-type cell at a fixed mother/daughter size ratio corresponding to ~30 min after bud emergence.

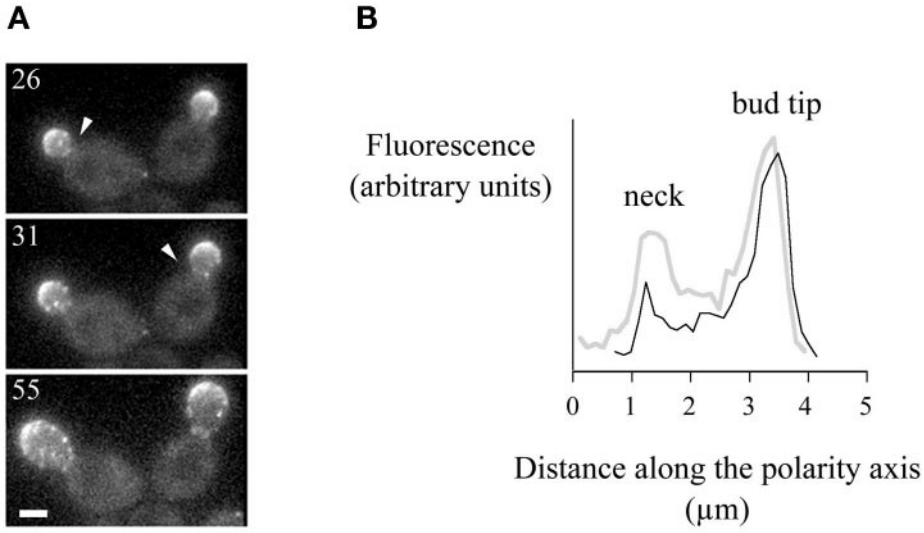

Figure 3. GFP-Bud6 localization in *bud3* haploids. (A) Selected frames from a 78-min time-lapse series showing the initial localization of GFP-Bud6 at the bud tip followed by faint label of the neck (arrowhead) in *bud3* cells (MYC4BG). The bulk of the label continued to associate with the distal bud surface as was the case in wild-type diploids. Numbers indicate time in minutes relative to bud emergence for the cell on the left. (B) Plot showing linescans through the polarity axis at 30 min after bud emergence in a *bud3* haploid cell. For reference, the labeling pattern of a wild-type haploid shown in Figure 2C has been overlaid (gray line).

2A). After bud emergence, label began to concentrate at the bud neck (Figure 2A, 15 min). Label intensity at the bud neck increased as the bud continued to grow, whereas label at the bud tip became scattered over the surface of the bud (Figure 2A, 42–61 min, left cell). Coincident with spindle disassembly, the bulk of label from the bud surface mobilized to the neck and gave rise to a double ring at cytokinesis (Figure 2A, 109–122 min, left cell). In diploids, Bud6 also associated sequentially with the bud surface and neck areas (Figure 2B). However, label in the bud remained primarily concentrated at the distal one-third of the bud surface, whereas the neck label was relatively less prominent (Figure 2B, 21–61 min). This contrasted with the scattered label of the bud surface and the relative bias of Bud6 label at the neck in haploids (Figure 2C).

Localization of the GFP-Bud6 fusion in *bud3*Δ haploid cells resembled that of wild-type diploids (Figure 3). A bias for concentration of label at the distal end of the bud and faint label at the neck was observed. Therefore, the haploid mode of Bud6 distribution requires Bud3 function.

In contrast, localization of GFP-Bud6 in *bni1*Δ mutants was disfavored at the bud tip surface relative to the neck area in both haploids and diploids (Figure 4A). Label at the neck appeared earlier relative to bud emergence (Figure 4B, 8–10 min) and prominent neck labeling occurred at a much smaller bud size than in wild-type cells (Figure 4, B and C). Thus, the bias for Bud6 distribution to the bud tip requires Bni1 function.

Accumulation of Bud6 at the neck began roughly with the timing of spindle assembly, raising the possibility that Bud6 may cue the sequential program of cytoplasmic microtubule interactions during SPB separation (Segal *et al.*, 2000). Moreover, the quantitative differences in Bud6 localization in haploids versus diploids correlated with the relative tendency to establish spindle–neck interactions observed in haploids. Finally, partitioning of Bud6 was affected by opposing cortical influences. Bud3, a protein essential for the axial budding pattern, forms a ring at the neck part-way through S phase both in haploids and diploids (Chant *et al.*, 1995), and may thus contribute to the more efficient association of Bud6 to this area in haploids. On the other hand, Bni1, essential for bipolar budding pattern in diploids, may promote the partition of Bud6 to the distal end of the bud.

Altered Program of Cytoplasmic Microtubule–Cortex Interactions during Spindle Assembly in Cortical Cue Mutants

To confirm the importance of Bud6 partition to the program of microtubule–cortex interactions responsible for spindle orientation, we examined *bud6* or *bni1* mutants expressing a GFP-Tub1 fusion to determine the relative role of bud tip versus bud neck interactions in spindle positioning and alignment during assembly.

After bud emergence, duplicated SPBs normally orient facing the bud neck with cytoplasmic microtubules interacting with the bud cortex (Byers and Goetsch, 1975; Shaw *et al.*, 1997; Segal *et al.*, 2000). In contrast to wild-type cells, *bud6* mutants were delayed in producing successful cytoplasmic microtubule interactions at this early step, resulting in an increase in cells that initiated spindle assembly away from the bud neck (Figure 5, A and B). This reflected a contribution of Bud6 at the bud tip during early phases of SPB orientation. The lack of early cytoplasmic microtubule–bud tip interactions and initiation of spindle assembly away from the bud neck disrupted the program of cytoplasmic microtubule interactions that normally determines one pole as daughter-bound (Shaw *et al.*, 1997; Segal *et al.*, 2000). However, microtubule capture eventually occurred when microtubules from one pole stochastically invaded the bud, inducing spindle alignment (Figure 5A, 23–29 min), followed by anaphase with virtually wild-type timing in 80% of cells (Figure 5A, 45–49 min). Thus, in spite of altered early orientation events, a *bud6* mutation caused a relatively mild defect in preanaphase spindle orientation, in terms of alignment along the polarity axis. These data also indicate that delayed microtubule-based search and capture into the bud could occur independently of Bud6 function. Indeed, analysis of *bud6 kar9* double mutants suggested that microtubule capture in the bud in a *bud6* context still relied on Kar9

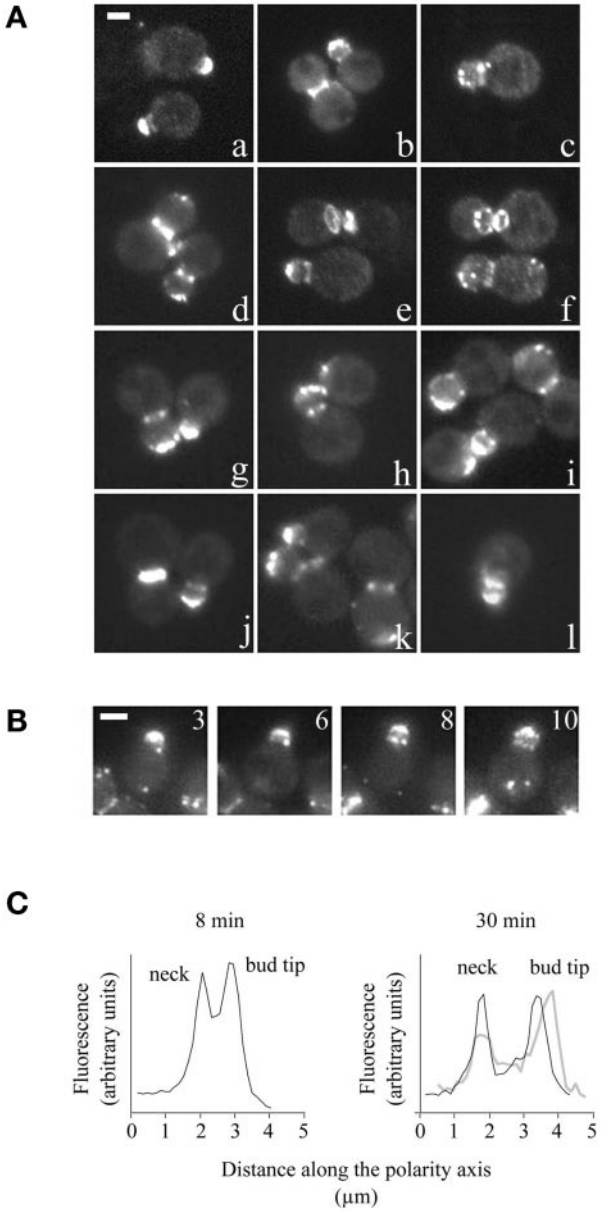

Figure 4. GFP-Bud6 localization in *bni1* mutants. (A) Localization of GFP-Bud6 in *bni1* haploid (MYC1BG; a–f) or *bni1/bni1* diploid (MYC11BG; g–l) cells. In *bni1*Δ haploid cells, Bud6 still associated to the prebud site (a) and showed discreet association to the neck region shortly after bud emergence (a, bottom). Small budded cells had prominent neck labeling (b, top; c; d, bottom cell). Label was relatively reduced and scattered at the bud tip of large budded cells (b, left; d, top; f). Neck label continued to be prominent after cytokinesis (e and f, top cells). In *bni1*Δ/*bni1*Δ diploid cells, Bud6 associated to the tip of the emerging bud (g, right). Yet, label became scattered on the bud tip surface unlike wild-type diploids (Figure 2B). Label, however was relatively prominent at the neck region (g–l). Bar, 2 μm. (B) Selected frames from a 20-min time-lapse series showing initial association to the neck area in a *bni1* haploid expressing a GFP-Bud6 fusion. Numbers indicate time elapsed in minutes relative to bud emergence. Bar, 2 μm. (C) Plot showing linescans through the polarity axis in a *bni1* haploid, indicating the relative label at the neck at 8 and 30 min after bud emergence. For reference, the label pattern of a wild-type haploid has been overlaid (gray line).

function (our unpublished results). Nevertheless, after microtubule capture in the bud, the newly assembled spindle remained loosely positioned at the bud neck and exhibited wide oscillations along the mother-bud axis (see below).

The compiled data from time-lapse analysis of early spindle orientation (n = 13) in combination with quantitation of spindle distribution by cell cycle stage and morphology (Figure 5B) indicated that 80% of *bud6* cells delayed orientation of side-by-side SPBs facing the bud neck relative to bud emergence. Twenty-two percent initiated spindle assembly away from the bud neck (1-μm-long spindles, distance to the neck >2 μm, no cytoplasmic microtubule contacts with the neck). In that case, orientation along the polarity axis, however, occurred as soon as cytoplasmic microtubules from one pole were captured by the bud, either during spindle assembly or shortly thereafter. As a result, only 8% of cells actually exhibited misaligned spindles immediately before anaphase (2-μm-long, >45° away from the polarity axis, no cytoplasmic microtubule interactions with the bud surface).

*bud6*Δ mutant defects were not restricted to early spindle orientation events (Figure 6). After correct alignment along the polarity axis, preanaphase spindles experienced wide oscillations (80% >3-μm distance from the neck, n = 15). Failure to properly retain the spindle at the neck accompanied a delay in anaphase onset or a pause (4 of 15 preanaphase spindles time lapsed; Figure 6A). In addition, *bud6*Δ cells were defective in confining cytoplasmic microtubules emanating from the $SPB_{daughter}$ to the bud. This consistently correlated with a delay in spindle disassembly (Figure 6B; notice the excessive curvature of the spindle in late anaphase, as previously described for *kip3*Δ cells by Straight *et al.*, 1998). These phenotypes emphasize the impact of Bud6-dependent functional microtubule–cortex interactions on correct spindle dynamics throughout the spindle pathway and underscore the importance of Bud6 at the bud surface and neck beyond early spindle orientation.

*bni1*Δ haploids displayed a seemingly more severe preanaphase spindle orientation defect in terms of alignment with respect to the mother-daughter axis. Orientation of side-by-side SPBs facing the emerging bud occurred abnormally early in this mutant (Figure 5, B and C). Spindles then tended to orient perpendicularly to the mother-daughter axis as a result of both poles interacting with the neck cortex (Figure 5C, large arrowheads). Because both poles primarily interacted with the neck during assembly, spindle polarity was impaired. This may explain the lack of pulling bias toward the bud and transits reported for spindles of the subpopulation of *bni1* cells experiencing a prolonged preanaphase delay (Lee *et al.*, 1999). Indeed, the *bni1*Δ mutation perturbed spindle dynamics and led to a significant delay in spindle elongation. Wild-type cells proceed to anaphase ~30 min after completing spindle assembly and alignment. In contrast, *bni1*Δ mutants exhibited a variable delay of 45–80 min before onset of anaphase.

The prevalence of microtubule–bud neck interactions correlated with the increased and premature association of Bud6 to the neck area observed in *bni1* mutants (Figure 4). Consistent with the role of Bud6 in mediating these interactions, *bni1*Δ *bud6*Δ double mutants showed a dramatic decrease in early SPB orientation and spindles positioned at the vicinity of the neck compared with *bni1*Δ single mutants

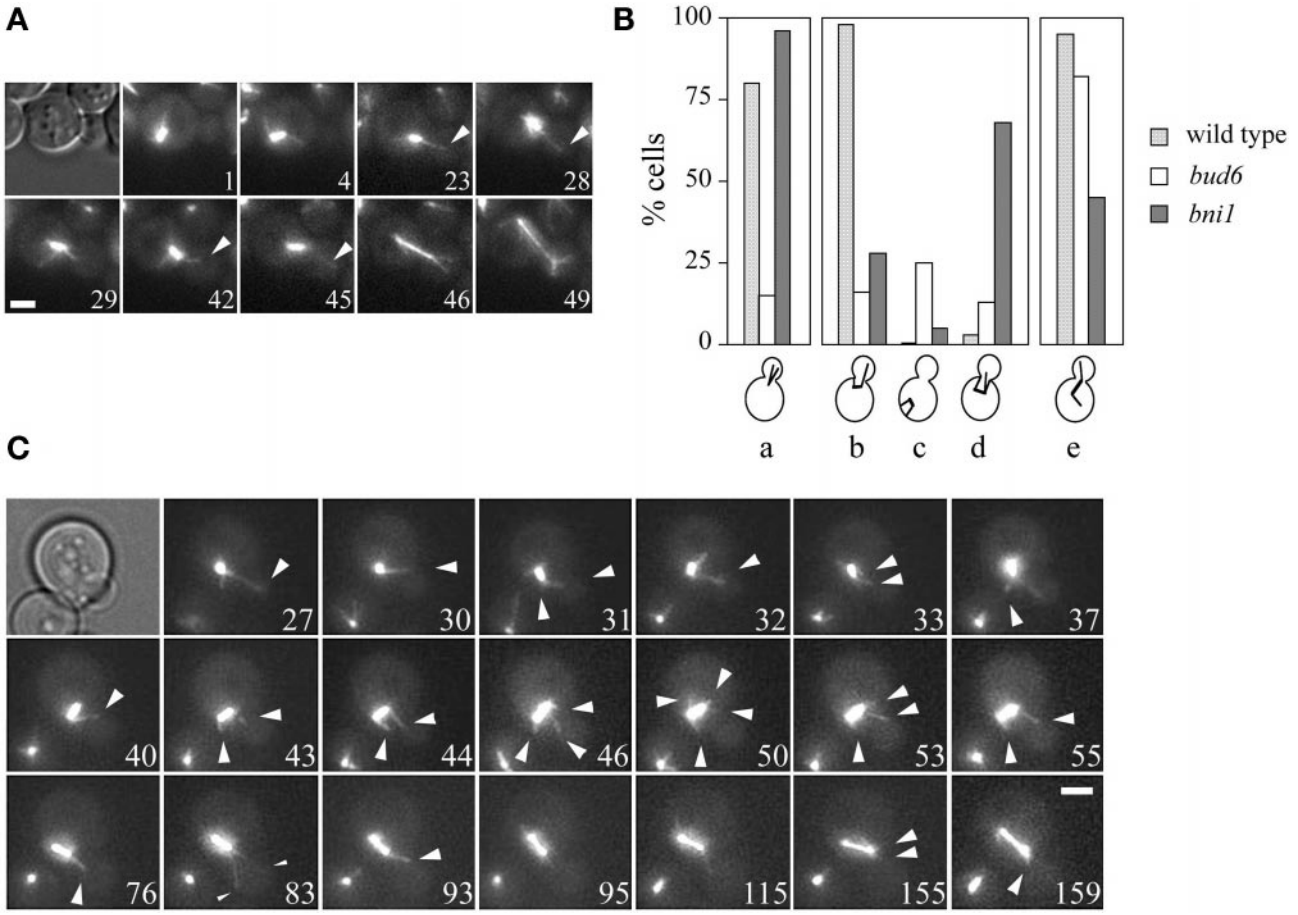

Figure 5. Cytoplasmic microtubule interactions and spindle orientation in cortical mutants during spindle morphogenesis. (A) Preanaphase spindle orientation in a *bud6* haploid expressing a GFP-Tub1 fusion (MYC2T). After spindle assembly away from the bud neck, cytoplasmic microtubule interactions occurred over the surface of the mother cell until microtubule capture by the bud cortex took place (28 min, arrowhead). These interactions brought about spindle alignment (42–45 min) before anaphase (46 min). (B) Distribution of spindle morphologies in wild-type, *bud6*, or *bni1* haploids. Cells expressing a GFP-Tub1 fusion were scored microscopically. Values represent the average of two counts of 500 cells at each stage depicted showing the indicated spindle morphology expressed as percentage: (a) oriented side by side SPB; (b) first step of spindle assembly, <1-μm-long spindle; (c) initial spindle assembly away from the neck; (d) both poles interacting with the neck; and (e) preanaphase orientation, <2-μm-long spindle. a, b, and e represent progressive steps of normal spindle development, whereas c and d represent aberrant configurations enriched in the mutant population. Spindles with observable cytoplasmic microtubule attachments from a single pole were included in the cell count at each stage but are not depicted as a category. (C) Cytoplasmic microtubule behavior during spindle assembly and orientation in a *bni1* haploid expressing a GFP-Tub1 fusion (MYC1T). After bud emergence, SPBs oriented facing the bud neck (27 min). At this stage already, microtubules appeared to interact primarily with the neck region (arrowheads). During spindle assembly, both poles interacted primarily with the neck (31–50 min). Interactions continued without clear definition of polarity until ~76 min. Eventually, the spindle became aligned with apparent microtubule interactions to the sides of the bud surface and neck (83 min, small arrowhead). Onset of anaphase occurred at 155 min. Numbers indicate time relative to bud emergence. Bar, 2 μm.

(Figure 7). As a result, the proportion of anaphases initiated in the mother cell was increased by 30%. Translocation of one SPB into the bud seemed frequently a consequence of being pushed through the bud neck as the spindle elongated in the mother cell.

Interestingly, *bni1*Δ diploids showed reduced bias for interactions with the bud neck area (20% ~1-μm-long spindles with both poles interacting with the bud neck) compared with *bni1*Δ haploids. The milder orientation impairment in *bni1*Δ diploids is consistent with less prevalent role of Bud6 in mediating cytoplasmic microtubule–neck interactions in diploids.

Kar9 has been suggested to participate in microtubule capture in the bud (Miller and Rose, 1998; Korinek *et al.*, 2000; Lee *et al.*, 2000). Our analysis indicated that neck interactions, on the other hand, seemed independent of Kar9 function. First, a *bni1*Δ *kar9*Δ haploid behaved similarly to a *bni1*Δ single mutant with regard to enhanced microtubule–bud neck interactions (Figure 7C). Therefore, spindle orientation in *bni1*Δ mutants resulted primarily from microtubule

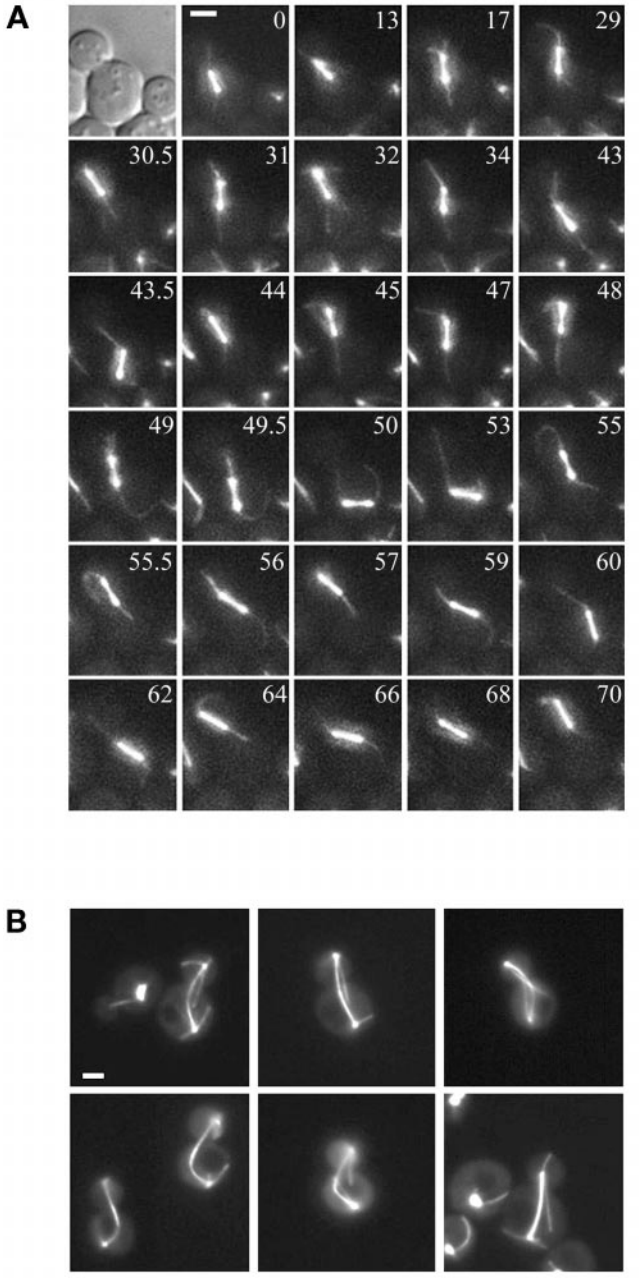

Figure 6. bud6Δ phenotypes at later stages of the spindle pathway. (A) Exaggerated spindle oscillations across the bud neck in a *bud6* haploid cell (MYC2T). In spite of correct alignment along the mother-bud axis, transits across the bud neck continued for at least 70 min after completion of spindle assembly. At the same time, spindle elongation paused at a length of 3.2 μm. (B) Cytoplasmic microtubule behavior of *bud6*Δ cells (MYC2T) in late anaphase. Microtubules emanating from the $SPB_{daughter}$ extend across the neck and into the mother cell. Late anaphase spindles are excessively long and tend to curve. Bars, 2 μm.

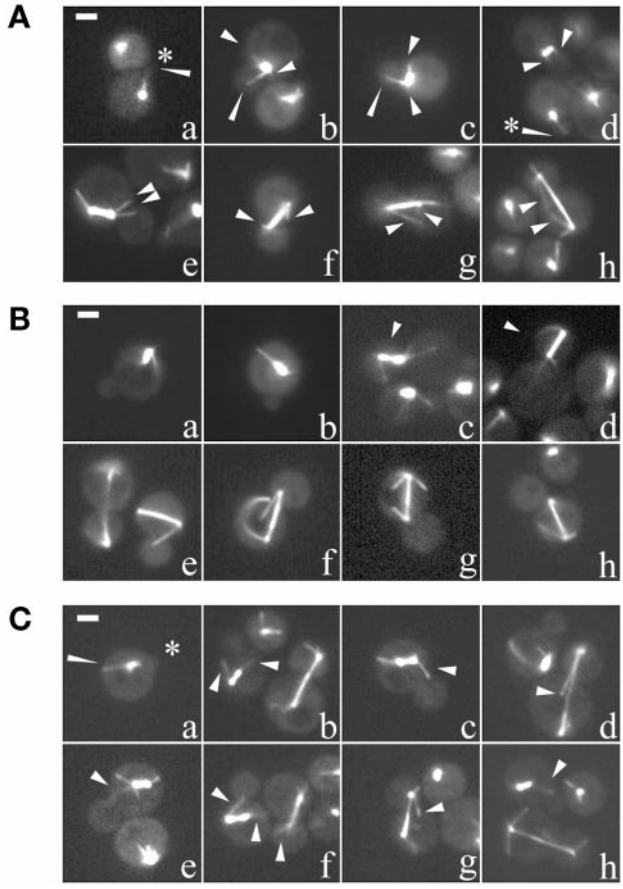

Figure 7. Effect of *bud6*Δ or *kar9*Δ in spindle orientation and neck interactions in *bni1*Δ haploids. Single fluorescence images of representative stages of spindle orientation and cytoplasmic microtubule behavior are shown. (A) *bni1* haploids (MYC1T): initial orientation of SPBs facing the bud (a and d, long arrowhead and asterisk). In cells containing short spindles, cytoplasmic microtubule interactions into the bud (b and c, long arrowhead) and to the neck (b–e, short arrowheads); persistent neck interactions during anaphase (f–h, arrowheads). (B) *bni1 bud6* haploids (MYC101T): early orientation of SPBs facing the bud and cytoplasmic microtubule attachments to the neck were suppressed. The orientation defect was more severe than in single *bud6* mutants. It is however difficult to factor out additional cytoskeletal defects that lead to a slow growth phenotype compared with either *bni1* or *bud6* single mutants. Short spindles away from the bud neck (a and b); mispositioned spindles in the bud reflecting lack of neck retention (c and d, arrows); anaphase spindles (e–h). (C) *bni1 kar9* haploids (MYC102T): initial orientation of SPBs facing the bud neck was delayed (a, arrowhead). As a result, the p of both poles interacting with the neck during spindle assembly was reduced compared with *bni1* single mutants (c and d, top cell). Cells with short spindles still oriented primarily by interactions with the neck (b, c, e, f, and h, top, arrowheads). Interactions persisted after onset of anaphase as in *bni1* cells (f, right cell; g). Bar, 2 μm.

attachments to the neck that appear to be Bud6 dependent and Kar9 independent. Yet, *bni1 kar9* double mutants showed a significant delay in SPB orientation facing the neck and cytoplasmic microtubule capture in the bud, relative to bud emergence, compared with *bni1* single mutants (Figures 5B and 7A). First, this indicated that Kar9 still contributed to spindle orientation in *bni1*Δ cells, irrespective of the effect of a *bni1*Δ mutation on Kar9 cortical localization reported pre-

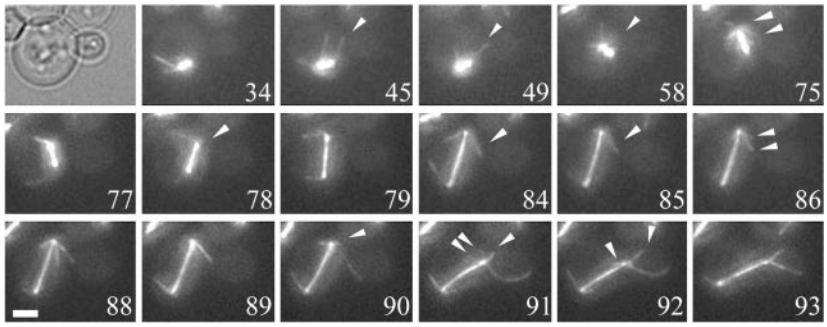

Figure 8. Neck interactions and spindle orientation during anaphase of a *kar9* haploid cell. Selected frames from a 100-min time-lapse series of a *kar9* cell expressing a GFP-Tub1 fusion (MYC3T). After spindle assembly, cytoplasmic microtubules interact with the vicinity of the neck (45–75 min, arrowheads) before onset of anaphase (77 min). Part way through anaphase, microtubules interacting with the neck (91–92 min, arrowheads) contribute to the translocation of one SPB into the bud. Numbers indicate time in minutes after bud emergence. Bar, 2 μm.

viously (Miller *et al.*, 1999). Second, analysis of otherwise wild-type *kar9*Δ cells showed that this mutant tended to initially assemble spindles away from the bud neck, consistent with a defect in early cytoplasmic microtubule capture by the bud cortex (Figure 8). However, eventual capture at the neck region (n = 5) appeared to create a situation permissive for initiation of spindle elongation in the mother cell (Figure 8, 75–86 min) and contributed to the translocation of one pole across the neck during anaphase in the absence of observable pulling force from the bud tip (Figure 8, 88–92 min). Thus, Kar9 is not required for cytoplasmic microtubule–neck interactions participating in spindle orientation.

Disruption of Spindle Polarity Provides a Sensitive Readout to Evaluate Cortical Cue Mutations

The relative importance of cytoplasmic microtubule–bud neck interactions in the orientation of the mitotic spindle was inferred initially from the distinct terminal positioning of a nonpolar spindle in diploid versus haploid *cdc28-4 clb5*Δ cells (Figure 1; Segal *et al.*, 1998). To directly test the role of cortical cues governing cytoplasmic microtubule interactions described above, we examined the genetic interaction between *cdc28-4 clb5*Δ and *bud6* or *bni1* mutations.

cdc28-4 clb5 bud6 haploid cells were inviable with full penetrance of the spindle-positioning defect characteristic of diploids (Figure 9, A and B). This result was reminiscent of the lethality of haploid *cdc28-4 clb5*Δ cells observed in combination with a *bud3*Δ mutation (Segal *et al.*, 1998). Because a *bud6* mutation does not modify the axial budding pattern of haploids, the positioning defect most likely reflects a direct requirement for Bud6 in the neck interactions needed to rescue a nonpolar spindle. In addition, the terminal positioning of nonpolar spindles in the bud induced by *bud6*Δ confirmed the presence of a residual bud-ward pulling force, consistent with a Bud6-independent, Kar9-dependent contribution to microtubule capture in the bud (Figure 5A).

cdc28-4 clb5 bni1 haploids or diploids had exaggerated microtubule interactions from both SPBs with the neck area consistent with enhanced partition of Bud6 to this region (Figure 9, C and D). As a consequence of the *bni1*Δ mutation, cytoplasmic microtubules interacted primarily with the neck throughout spindle assembly, irrespective of SPB identity. These interactions increased retention of the spindle at the neck until anaphase was initiated. Retention of the spindle at the neck correlated with the suppression of diploid lethality and the ability of cells to progress into anaphase (Figure 9, C–E). A *bni1*Δ mutation could not increase neck interactions in the absence of Bud6. Thus, Bud6-dependent enhancement of neck interactions was consistent with the GFP-Bud6 accumulation at the neck observed in *bni1*Δ haploids or diploids (Figure 4).

In conclusion, deletion of *BUD6* abrogated the differential contribution of cytoplasmic microtubule–neck interactions that can otherwise rescue spindle positioning in haploids. Conversely, deletion of *BNI1* suppressed the lethality arising from symmetric spindle formation in diploids. Thus, although disruption of inherent spindle polarity occurred with full penetrance both in haploids and diploids (Figure 1; Segal *et al.*, 2000), the terminal positioning of the spindle was dictated by differential distribution of cortical cues normally directing cytoplasmic microtubule contacts in haploids relative to diploids.

DISCUSSION

Dual Localization of Bud6 and the Temporal Program of Microtubule–Cortex Interactions during Spindle Assembly

Stepwise cytoplasmic microtubule contacts, first with the bud tip, and then with the bud neck during spindle morphogenesis, underlie the program imparting correct spindle polarity and orientation (Shaw *et al.*, 1997; Segal *et al.*, 2000). Bud6, a protein implicated in bud site selection and spindle orientation, has the remarkable property of localizing sequentially to the bud tip and the bud neck (Figure 2; Amberg *et al.*, 1997). Such behavior is compatible with a role in directing the program of cytoplasmic microtubule–cortex interactions during spindle assembly. The genetic and cytological analysis presented here strongly favors this view.

First, a striking correlation was observed between the relative abundance of Bud6 at the bud neck and the promotion of microtubule–bud neck interactions in haploids versus diploids (Figure 2). Second, a *bud6* mutation impaired early SPB orientation and dramatically reduced cytoplasmic microtubule–bud neck interactions during spindle assembly in otherwise wild-type cells (Figure 5). Finally, Bud6 partition between the bud tip and the neck could be influenced by cortical mutations that also affect bud site selection (Figures 3 and 4). The effect of these mutations on the relative distribution of Bud6 to the neck correlated precisely with an enhancement or a decrease in microtubule–bud neck contacts in a Bud6-dependent manner (Figures 5–7). The biological impact of these effects was confirmed by using the spindle-positioning defect and lethality arising from *cdc28-4*

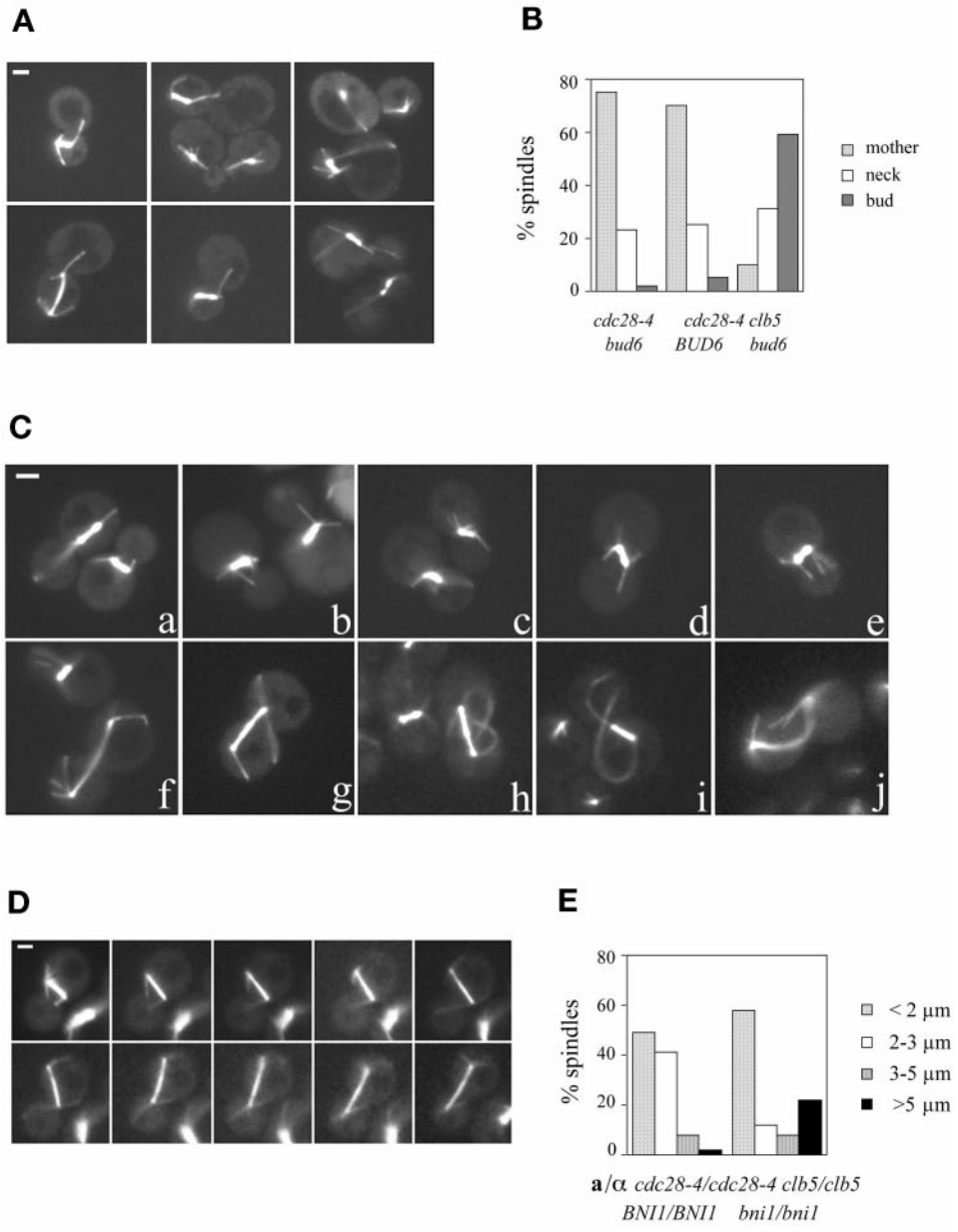

Figure 9. Effect of cortical mutations in the penetrance of a spindle-positioning defect resulting from disruption of inherent spindle polarity (*cdc28-4 clb5*Δ cells). (A) Spindle positioning in *cdc28-4 clb5 bud6 GAL:CLB5* haploids (MY16CTC2) after a 6-h shift of an asynchronous culture to glucose-containing medium. Representative spindle morphologies, as visualized by using a *GFP-TUB1* construct, are shown. Single images were captured by using 100% fluorescence intensity and 500-ms exposures as previously described (Segal *et al*., 1998). (B) Spindle distribution by position for *cdc28-4 clb5* (MY16CT), *cdc28-4 bud6* (MY10CC2T), or *cdc28-4 clb5 bud6* (MY16CTC2) mutant is shown. Scores represent the average of three sets of 500 cells counted containing short, <2.5-μm-long spindles (85% of cells containing a spindle for the triple mutant). (C) Spindle positioning in *cdc28-4 clb5 bni1 GAL1:CLB5* diploids (MYT1614C1) after a 6-h shift to glucose-containing medium. The *bni1* mutation could correct spindle positioning at least in two ways: the mutation may suppress the initial tendency of cytoplasmic microtubules from either pole to reach the bud tip during spindle assembly (a and b) or increase the interactions to the neck area (c–f). Exaggerated interactions with the neck region continued after onset of anaphase (g–j). Bar, 2 μm. (D) A *cdc28-4 clb5 bni1* diploid initiated anaphase, whereas both spindle poles interacted with the neck. Frames are 2 min apart. Bar. 2 μm. (E) Effect of the *bni1* mutation on spindle distribution by length showing increased anaphase spindles in the triple mutant. Spindle measurements in digital images were carried out as previously described (Segal *et al*., 1998). Spindle translocation in the bud was reduced from 65 to 9% in the triple mutant.

*clb5*Δ double mutation (Segal *et al*., 1998) as a readout. A *bni1*Δ mutation directed Bud6 to the neck region (Figure 4) and rescued the lethality associated with *cdc28-4 clb5* diploids (Figure 8). Conversely, *bud3*Δ reduced Bud6 partitioning to the neck conferring lethality to *cdc28-4 clb5* haploids (Figure 3; Segal *et al*., 1998).

Thus, a general model for spindle assembly and orientation can be proposed based on our original suggestion that a Clb5-dependent delay in cytoplasmic microtubule organization (Segal *et al*., 2000) translates into correct fate of the SPB_{mother} (Figure 10A). The model incorporates the role of Bud6 in orienting functional cytoplasmic microtubule attachments. Timely capture of microtubules emanating from the bridge at the bud cortex (a process contributed to by both Kar9 and Bud6) directs orientation of duplicated SPBs so that they face the bud neck (Figure 10Aa). At the onset of SPB separation, the $SPB_{daughter}$ inherits these microtubule contacts (Figure 10Ab). Concomitant with formation of a short spindle, a second area of Bud6-dependent interactions appears at the bud neck (Figure 10Ac). Thus, de novo microtubules are restricted to interact with the bud neck region and prevented from undergoing capture in the bud. These new interactions result in correct fate of the SPB_{mother} and retention of the preanaphase spindle at the neck (Figure 10Ad–f). This step in the process of establishment of spindle polarity accounts for the necessity for a dual mechanism of microtubule capture relying on, at least, two independent components. The timely appearance of Bud6 at the neck directs new contacts (a Kar9-independent process) without

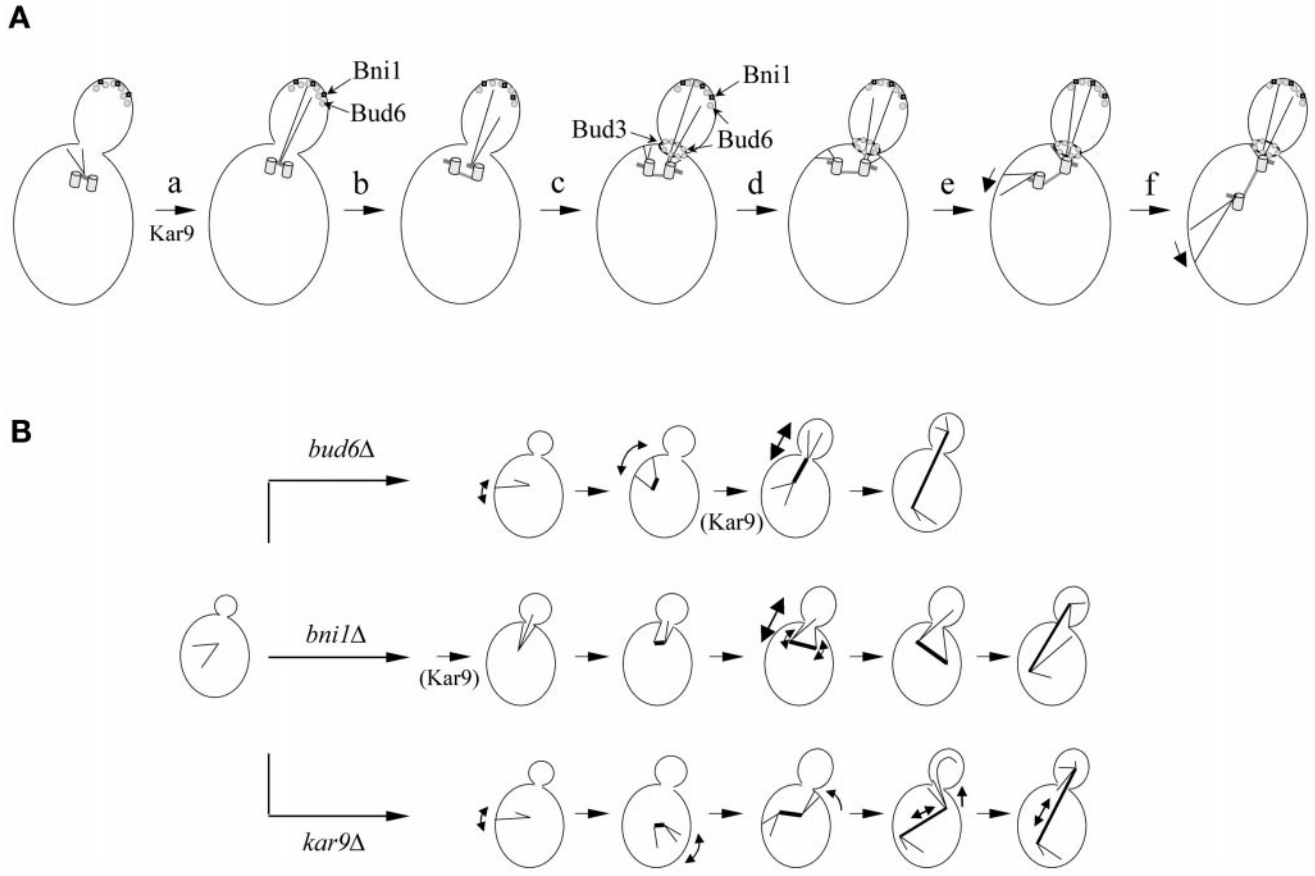

Figure 10. A model for Bud6's role in directing the program of cytoplasmic microtubule interactions during spindle assembly. (A) After bud emergence, positional information at the bud tip directs microtubule interactions, thereby orienting duplicated SPBs facing the bud neck (a). As SPBs separate, the $SPB_{daughter}$ retains contacts to the bud tip (b). In concert with spindle assembly, de novo cytoplasmic microtubules are directed to a new Bud6-dependent area of capture at the neck and prevented from undergoing capture in the bud (c). As spindle assembly proceeds, cytoplasmic microtubule interactions draw the SPB_{mother} away from the neck and cause spindle alignment (d and f). Neck interactions also contribute to spindle retention at the neck. Premature organization of cytoplasmic microtubules in *cdc28-4 clb5* cells (Segal *et al.*, 2000) favors de novo contacts with the bud tip before an area for cytoplasmic microtubule–bud neck interactions develops. Bud6 partition between the bud tip and neck is influenced by Bni1 and Bud3, respectively. (B) Alternative modes of spindle orientation in cortical cue mutants. A *bud6* mutation impairs initial orientation of duplicated SPBs facing the bud neck and ensuing neck interactions. Orientation relies primarily on microtubule search and capture by the bud. A *bni1* mutation directs interactions to the neck throughout spindle morphogenesis. In both mutants, Kar9 still contributes to orientation. On the other hand, a *kar9* mutation reduces cytoplasmic microtubule capture in the bud while orientation via neck interactions can occur after spindle assembly (when Bud6 accumulates at the neck) or during anaphase.

perturbing early functional attachments with the bud. Accordingly, a delay in microtubule organization relative to SPB separation, under cyclin-dependent kinase control (Segal *et al.*, 2000), in concert with the appearance of this new area for enhanced microtubule–cortex interactions at the neck defines the temporal window in which establishment of correct spindle polarity takes place (Segal *et al.*, 1998, 2000).

Spindle Orientation Defect in bni1 *Cells Reflects the Importance of Bud6 Partition in Cytoplasmic Microtubule–Cortex Interactions*

Bni1 is a member of the formin family, including proteins implicated in a variety of processes ranging from cytokinesis to asymmetric segregation of developmental determinants (Woychik *et al.*, 1990; Jansen *et al.*, 1996; Harris *et al.*, 1997; Beach *et al.*, 1999). Additionally, a *bni1*Δ results in a pronounced defect in spindle orientation and dynamics. We propose that this effect is primarily mediated by a relative bias for Bud6 localization to the neck after bud emergence. This bias caused excessive cytoplasmic microtubule contacts with the neck area early in the spindle pathway (Figures 4 and 5), in a Kar9-independent manner (Figure 7) and continued even after onset of anaphase (Figures 5 and 7). A *bud6*Δ mutation eliminated these excessive interactions, confirming the role of Bud6 in directing these microtubule contacts (Figure 7). Accordingly, both bud site selection and spindle orientation functions are disrupted in *bni1* alleles defective in interaction with Bud6 (Lee *et al.*, 1999). Instead,

although Kar9-dependent microtubule capture in the bud still contributed to orientation in *bni1*Δ cells, deletion of *KAR9* did not cancel the excessive neck interactions occurring in this background (Figure 6C). Therefore, it is unlikely that the effects of *bni1*Δ are mediated by Kar9 mislocalization away from the bud tip as previously proposed (Lee *et al.*, 1999; Miller *et al.*, 1999). In fact, a Kar9-GFP fusion still localized to cytoplasmic microtubules in *bni1*Δ or *bud6*Δ mutants as in wild-type cells consistent with proficient Kar9-dependent microtubule capture in the bud (our unpublished results). More importantly, *bni1*Δ and *kar9*Δ mutations have, in addition, distinct impact on overall spindle dynamics and temporal program of cytoplasmic microtubule attachments to the bud tip and neck regions (Figures 5 and 8). *bni1*Δ cells experience a prolonged delay in onset of anaphase, whereas *kar9*Δ cells initiate anaphase approximately on schedule. Such behavior makes it unlikely that *bni1*Δ phenotypes rely heavily on disruption of Kar9 function.

Taken together, these observations underscore the importance of Bud6 temporal partition in promotion of cytoplasmic microtubule interactions first with the bud and then with the neck region to direct the program for establishment of spindle polarity. By affecting temporal and quantitative partition of Bud6, a *bni1*Δ mutation encourages spindle orientation primarily on the basis of neck interactions, thus disrupting correct spindle polarity and dynamics.

A Complementary View of Nuclear Migration and Spindle Orientation

The analysis of mutations that affect spindle development and function has led to the initial assignment of pairs of motor activities and cortical cues arranged in putative early and late pathways required for nuclear migration and spindle orientation (Heil-Chapdelaine *et al.*, 1999). This model, however, cannot account for the establishment of correct SPB identity (beyond cytoplasmic microtubule capture in the bud) as well as the retention of the spindle at the neck with low mobility before anaphase (Yeh *et al.*, 1995). These earlier studies paradoxically assigned a relatively minor role to Bud6 in spindle positioning. In contrast, the present study indicates that temporal partition of Bud6 may be critical for spindle orientation (Figures 4 and 5), and that a *bud6*Δ mutation can significantly disrupt functional microtubule–cortex interactions throughout the spindle pathway with concomitant impact on spindle dynamics (Figures 5 and 6).

We therefore offer a complementary view of the process of spindle orientation, based on the relative participation of bud tip and neck areas in the establishment of spindle polarity during assembly, as reflected in the altered modes of spindle orientation in response to single cortical cue mutations (Figure 10B). This view emerged by observation of the entire process of spindle assembly and orientation, not factored into the previous studies. In this light, for example, *kar9 dhc1* synthetic lethality (Miller and Rose, 1998) may be due to the fact that SPB translocation in *kar9* cells relies heavily on microtubule–bud neck interactions, which are compromised by *dhc1*Δ. A *dhc1*Δ mutation causes hyperstable neck interactions suggesting that dynein-driven microtubule instability is particularly critical for transient neck contacts (our unpublished results). Similarly, *bni1 dhc1* synthetic lethality (Miller *et al.*, 1999) can be explained by the fact that excessive cytoplasmic microtubule contacts to the bud neck in a *bni1*Δ mutant depend on dynein-mediated dynamic instability to permit spindle orientation. In both of these examples, cortical mutations sensitize spindle orientation to impairment of cytoplasmic microtubule dynamics. Thus, genetic interactions with mutations disrupting motor functions, such as *dhc1*Δ, do not lend themselves to the classical genetic approach of epistasis analysis and assignment to functional pathways. *bni1*Δ *dhc1*Δ or *kar9*Δ *dhc1*Δ synthetic lethality does not imply that Bni1 and Kar9 participate in the same pathway. Indeed, the spindle defects in a *bni1*Δ *kar9*Δ double mutant are very different from those in the single mutants (Figures 5–8) and indicate that Bni1 and Kar9 contribute separately to the cytoplasmic microtubule program resulting in spindle orientation. These differential contributions, however, may not be apparent when genetic analysis is performed evaluating phenotypes on the basis primarily of nuclear position by 4,6-diamidino-2-phenylindole (DAPI) staining.

Equally susceptible to alternative interpretation is the assignment of Kip3 as the motor mediating early orientation. Lee *et al.* (1999) proposed that Kip3 and Bni1 must participate in a common pathway because the respective mutations share related phenotypes and do not interact genetically. However, in agreement with Straight *et al.* (1998) we found that *kip3*Δ mutants are overtly impaired in spindle disassembly upon mitotic exit, which may interfere with onset of characteristically high microtubule instability critical for early SPB orientation facing the bud neck (Carminati and Stearns, 1997; Tirnauer *et al.*, 1999). Indeed, an *ase1*Δ mutation suppresses the extended anaphase of *kip3*Δ cells and concomitantly reverts the nuclear migration phenotype (Segal and Reed, unpublished results). In contrast, *ase1*Δ and *bni1*Δ mutations exhibit synthetic lethality (Lee *et al.*, 1999). Thus, it is unlikely that Kip3 and Bni1 share a direct role in early orientation. Again, evaluation of phenotypes on the basis of microtubule dynamics is helpful in clarifying relationships previously established primarily on the basis of nuclear positioning.

A Link between Bud Site Selection and Spindle Orientation in Yeast

We previously reported a connection between bud site selection and spindle orientation (Segal *et al.*, 1998). Based on the present study, this link manifests in the relative contribution of the neck region to both spindle orientation and the axial budding pattern of haploids. Although haploids, specialized for mating functions, may exploit a common machinery for partition of determinants controlling mating-type switching, polarized growth, and for tethering nuclei to the neck, diploids (budding bipolarly) may require increased bias of pulling force into the daughter cell for effective SPB translocation. Indeed, axial budding relies on transient signals, whereas bipolar budding responds to persistent or perhaps permanent signals (Chant and Pringle, 1995). In the latter case, it might be necessary to suppress the contribution of neck interactions over bud-ward forces to facilitate unequivocal segregation of one SPB into the newly formed bud.

Nevertheless, a tight link between the axis of division, as defined by the site of bud emergence, and spindle orientation is not essential for yeast viability. Cells can adopt more convoluted pathways (Figure 10B) to achieve correct nuclear

division irrespective of the site of bud emergence. Yet, this may not adequately reflect the biological significance of efficient spindle orientation. In yeast, early commitment of $SPB_{daugther}$ and SPB_{mother} ensures that spindle assembly and orientation are complete within roughly 1 h. Loss of polarity causes variable delays in preanaphase time (*bni1*, *cdc28-4 clb5*, etc.) or during anaphase (*dhc1*, *kar9*, *bud6*, etc.). Although these delays may be tolerated in a unicellular organism, they could still compromise fitness in the wild. In contrast, metazoan embryonic systems depending on division speed, asymmetry as a means to generate cell diversity, or inability to execute checkpoint-mediated delays must rely on perfect coupling of spindle orientation and division to ensure viability of the organism as a whole, under any conditions. These systems specify the division plane based on the orientation of the spindle. Thus, positional cues direct both spindle positioning and secondarily the division axis. Wild-type yeast cells may follow a similar principle. Rather than aligning the spindle according to a prespecified axis of division, cells couple both processes based on the use of common determinants directing budding pattern and spindle orientation.

ACKNOWLEDGMENTS

We thank A.F. Straight and M. Longtine for generous gift of plasmids and strains. Thanks to P. Maddox for assistance with digital microscopy, D.J. Clarke for stimulating discussions and critical reading of the manuscript, and members of the Reed, Wittenberg, Russell, Bloom, and Salmon labs for the supporting environment. This work was supported by a United States Public Health Service grant GM-38328 to S.I.R.

REFERENCES

Amberg, D.C., Zahner, J.E., Mulholland, J.W., Pringle, J.R., and Botstein, D. (1997). Aip3p/Bud6p, a yeast actin-interacting protein that is involved in morphogenesis and the selection of bipolar budding sites. Mol. Biol. Cell *8*, 729–753.

Beach, D.L., Salmon, E.D., and Bloom, K. (1999). Localization and anchoring of mRNA in budding yeast. Curr. Biol. *9*, 569–578.

Byers, B. (1981). Cytology of the yeast life cycle. In: The Molecular Biology of the Yeast *Saccharomyces*: Life Cycle and Inheritance, ed. J.N. Strathern, E.W. Jones, and J.R. Broach, Cold Spring Harbor, NY: Cold Spring Harbor Press, 59–96.

Byers, B., and Goetsch, L. (1975). Behavior of spindles and spindle plaques in the cell cycle and conjugation of *Saccharomyces cerevisiae.* J. Bacteriol. *124*, 511–523.

Carminati, J.L., and Stearns, T. (1997). Microtubules orient the mitotic spindle in yeast through dynein-dependent interactions with the cell cortex. J. Cell Biol. *138*, 629–641.

Chant, J., and Herskowitz, I. (1991). Genetic control of bud site selection in yeast by a set of gene products that constitute a morphogenetic pathway. Cell *65*, 1203–1212.

Chant, J., Mischke, M., Mitchell, E., Herskowitz, I., and Pringle, J.R. (1995). Role of Bud3p in producing the axial budding pattern of yeast. J. Cell Biol. *129*, 767–778.

Chant, J., and Pringle, J.R. (1995). Patterns of bud site selection in the yeast *Saccharomyces cerevisiae.* J. Cell Biol. *129*, 751–765.

Eshel, D., Urrestarazu, L.A., Vissers, S., Jauniaux, J.C., van Vliet-Reedijk, J.C., Planta, R.J., and Gibbons, I.R. (1993). Cytoplasmic dynein is required for normal nuclear segregation in yeast. Proc. Natl. Acad. Sci. USA *90*, 11172–11176.

Evangelista, M., Blundell, K., Longtine, M.S., Chow, C.J., Adames, N., Pringle, J.R., Peter, M., and Boone, C. (1997). Bni1p, a yeast formin linking Cdc42p and the actin cytoskeleton during polarized morphogenesis. Science *276*, 118–122.

Farkasovsky, M., and Kuntzel, H. (1995). Yeast Num1p associates with the mother cell cortex during S/G2 phase and affects microtubular functions. J. Cell Biol. *131*, 1003–1014.

Fujiwara, T., Tanaka, K., Mino, A., Kikyo, M., Takahashi, K., Shimizu, K., and Takai, Y. (1998). Rho1p-Bni1p-Spa2p interactions: implication in localization of Bni1p at the bud site and regulation of the actin cytoskeleton in *Saccharomyces cerevisiae.* Mol. Biol. Cell *9*, 1221–1233.

Harris, S.D., Hamer, L., Sharpless, K.E., and Hamer, J.E. (1997). The *Aspergillus nidulans sepA* gene encodes an FH1/2 protein involved in cytokinesis and the maintenance of cellular polarity. EMBO J. *16*, 3474–3483.

Heil-Chapdelaine, R.A., Adames, N.R., and Cooper, J.A. (1999). Formin' the connection between microtubules and the cell cortex. J. Cell Biol. *144*, 809–811.

Hoyt, M.A., and Geiser, J.R. (1996). Genetic analysis of the mitotic spindle. Annu. Rev. Genet. *30*, 7–33.

Imamura, H., Tanaka, K., Hihara, T., Umikawa, M., Kamei, T., Takahashi, K., Sasaki, T., and Takai, Y. (1997). Bni1p and Bnr1p: downstream targets of the Rho family small G-proteins which interact with profilin and regulate actin cytoskeleton in *Saccharomyces cerevisiae.* EMBO J. *16*, 2745–2755.

Jansen R.-P., Dowser, C., Michaelis, C., Galova, M., and Nasmyth, K. (1996). Mother cell-specific HO expression in budding yeast depends on the unconventional myosin Myo4p and other cytoplasmic proteins. Cell *84*, 687–697.

Kohno, H., Tanaka, K., Mino, A., Mino, M., Umikawa, M., Imamura, H., Fujiwara, T., Fujita, Y., Hotta, K., Qadota, H., Watanabe, T., Ohya, Y., and Takai, Y. (1996). Bni1p implicated in cytoskeletal control is a putative target of Rho1p small G.T.P. binding protein in *Saccharomyces cerevisiae.* EMBO J. *15*, 6060–6068.

Korinek, W.S., Copeland, M.J., Chaudhuri, A., and Chant, J. (2000) Molecular linkage underlying microtubule orientation toward cortical sites in yeast. Science *287*, 2257–2259.

Lee, L., Klee, S.K., Evangelista, M., Boone, C., and Pellman, D. (1999). Control of mitotic spindle position by the *Saccharomyces cerevisiae* formin Bni1p. J. Cell Biol. *144*, 947–961.

Lee, L., Tirnauer, J.S., Li, J., Schuyler, S.C., Liu, J.Y., and Pellman, D. (2000). Positioning of the mitotic spindle by a cortical microtubule capture mechanism. Science *287*, 2260–2262.

Lew, D.J., Weinert, T., and Pringle, J.R. (1997). Cell cycle control in *Saccharomyces cerevisiae.* In: The Molecular and Cellular Biology of the Yeast *Saccharomyces*, ed. J.R. Pringle, J.R. Broach, and E.W. Jones, Cold Spring Harbor, NY: Cold Spring Harbor Laboratory Press, 607–695.

Li, Y.Y., Yeh, E., Hays, T., and Bloom, K. (1993). Disruption of mitotic spindle orientation in a yeast dynein mutant. Proc. Natl. Acad. Sci. USA *90*, 10096–10100.

Maddox, P., Chin, E., Mallavarapu, A., Yeh, E., Salmon, E.D., and Bloom, K. (1999). Microtubule dynamics from mating through the first zygotic division in the budding yeast *Saccharomyces cerevisiae*. J. Cell Biol. *144*, 977–987.

Miller, R.K., Matheos, D., and Rose, M.D. (1999). The cortical localization of the microtubule orientation protein, Kar9p, is dependent upon actin and proteins required for polarization. J. Cell Biol. *144*, 963–975.

Miller, R.K., and Rose, M.D. (1998). Kar9p is a novel cortical protein required for cytoplasmic microtubule orientation in yeast. J. Cell Biol. *140*, 377–390.

Rhyu, M.S., and Knoblich, J.A. (1995). Spindle orientation and asymmetric cell fate. Cell *82*, 523–526.

Segal, M., Clarke, D.J., Maddox, P., Salmon, E.D., Bloom, K., and Reed, S.I. (2000). Coordinated spindle assembly and orientation requires Clb5p-dependent kinase in budding yeast. J. Cell Biol. *148*, 441–452.

Segal, M., Clarke, D.J., and Reed, S.I. (1998). Clb5-associated kinase activity is required early in the spindle pathway for correct preanaphase nuclear positioning in *Saccharomyces cerevisiae.* J. Cell Biol. *143*, 135–145.

Shaw, S.L., Yeh, E., Maddox, P., Salmon, E.D., and Bloom, K. (1997). Astral microtubule-based searching mechanism for spindle orientation and nuclear migration into the bud. J. Cell Biol. *139*, 985–994.

Sherman, F., Fink, G., and Hicks, J.B. (1986). Methods in Yeast Genetics. Cold Spring Harbor, NY: Cold Spring Harbor Laboratory.

Straight, A.F., Marshall, W.F., Sedat, J.W., and Murray, A.W. (1997). Mitosis in living budding yeast: anaphase A but no metaphase plate. Science *277*, 574–578.

Straight, A.F., Sedat, J.W., and Murray, A.W. (1998). Time-lapse microscopy reveals unique roles for kinesins during anaphase in budding yeast. J. Cell Biol. *143*, 687–694.

Tirnauer, J.S., O'Toole, E., Berrueta, L., Bierer, B.E., and Pellman, D. (1999). Yeast Bim1p promotes the G1-specific dynamics of microtubules. J. Cell Biol. *145*, 993–1007.

Vallen, E.A., Scherson, T.Y., Roberts, T., van Zee, K., and Rose, M.D. (1992). Asymmetric mitotic segregation of the yeast spindle pole body. Cell *69*, 505–515.

Wach, A., Brachat, A., Pohlmann, R., and Philippsen, P. (1994). New heterologous modules for classical or PCR based gene disruptions in *Saccharomyces cerevisiae.* Yeast *10,* 1793–1808.

Woychik, R.P., Maas, R.L., Zeller, R., Vogt, T.F., and Leder, P. (1990). "Formins": proteins deduced from the alternative transcripts of the limb deformity gene. Nature *346*, 850–853.

Yeh, E., Skibbens, R.V., Cheng, J.W., Salmon, E.D., and Bloom, K. (1995). Spindle dynamics and cell cycle regulation of dynein in the budding yeast *Saccharomyces cerevisiae.* J. Cell Biol. *130,* 687–700.

Zahner, J.E., Harkins, H.A., and Pringle, J.R. (1996). Genetic analysis of the bipolar pattern of bud site selection in the yeast *Saccharomyces cerevisiae.* Mol. Cell. Biol. *16*, 1857–1870.